AFRL-RQ-WP-TR-2019-0016

3D PRINTED MOTOR

In-house Seedling Effort: Experiential Training for Building and Experimentally Testing a Motor Using 3D Printed Elements

Kevin J. Yost
Electrical Systems Branch
Power and Control Division

Maxwell Stelmack
Wright Scholar Research Assistant Intern

FEBRUARY 2019
Interim Report

AIR FORCE RESEARCH LABORATORY
AEROSPACE SYSTEMS DIRECTORATE
WRIGHT-PATTERSON AIR FORCE BASE, OH 45433-7542
AIR FORCE MATERIEL COMMAND
UNITED STATES AIR FORCE

NOTICE AND SIGNATURE PAGE

Using Government drawings, specifications, or other data included in this document for any purpose other than Government procurement does not in any way obligate the U.S. Government. The fact that the Government formulated or supplied the drawings, specifications, or other data does not license the holder or any other person or corporation; or convey any rights or permission to manufacture, use, or sell any patented invention that may relate to them.

This paper was cleared for public release by the USAF 88th Air Base Wing (88 ABW) Public Affairs Office (PAO) and is available to the general public, including foreign nationals.

Qualified requestors may obtain copies of this report from the Defense Technical Information Center (DTIC) (http://www.dtic.mil).

AFRL-RQ-WP-TR-2019-0016 has been reviewed and is approved for publication in accordance with assigned distribution statement.

This report is published in the interest of scientific and technical information exchange and its publication does not constitute the Government's approval or disapproval of its ideas or findings.

REPORT DOCUMENTATION PAGE

Form Approved
OMB No. 0704-0188

1. REPORT DATE *(DD-MM-YY)*	2. REPORT TYPE	3. DATES COVERED *(From - To)*
February 2019	Interim	04 February 2017 – 04 February 2019

4. TITLE AND SUBTITLE
3D PRINTED MOTOR
In-house Seedling Effort: Experiential Training for Building and Experimentally Testing a Motor Using 3D Printed Elements

5a. CONTRACT NUMBER
In-house

5b. GRANT NUMBER

5c. PROGRAM ELEMENT NUMBER
62203F

6. AUTHOR(S)
Kevin J. Yost (AFRL/RQQE)
Maxwell Stelmack (Wright Scholar Research Assistant Intern)

5d. PROJECT NUMBER
3145

5e. TASK NUMBER

5f. WORK UNIT NUMBER
Q1G2

7. PERFORMING ORGANIZATION NAME(S) AND ADDRESS(ES)
Electrical Systems Branch (AFRL/RQQE)
Power and Control Division
Air Force Research Laboratory, Aerospace Systems Directorate
Wright-Patterson Air Force Base, OH 45433-7542
Air Force Materiel Command
United States Air Force

8. PERFORMING ORGANIZATION REPORT NUMBER
AFRL-RQ-WP-TR-2019-0016

9. SPONSORING/MONITORING AGENCY NAME(S) AND ADDRESS(ES)
Air Force Research Laboratory
Aerospace Systems Directorate
Wright-Patterson Air Force Base, OH 45433-7542
Air Force Materiel Command
United States Air Force

10. SPONSORING/MONITORING AGENCY ACRONYM(S)
AFRL/RQQE

11. SPONSORING/MONITORING AGENCY REPORT NUMBER(S)
AFRL-RQ-WP-TR-2019-0016

12. DISTRIBUTION/AVAILABILITY STATEMENT
DISTRIBUTION STATEMENT A. Approved for public release. Distribution is unlimited.

13. SUPPLEMENTARY NOTES
PA Clearance Number: 88ABW-2018-5700; Clearance Date: 13 OCT 18

14. ABSTRACT
3D printing and additive manufacturing (AM) are rapidly growing technical areas. More affordable options and capability advancements increase the attraction for exploring innovative methods. The potential performance and cost saving benefits indicate AM is a prospective disruptive technology over traditional manufacturing methods. However, there are significant challenges that exist within the breadth of methods and material options. Simple, low cost, and quick projects, i.e. a technical sprint, develop relevant experience prior to investing into higher cost and vital projects. This report covers results and lessons learned from an eight week technical sprint effort. The effort explored various technical areas and challenges needed in order to more proficiently explore AM for electric machines such as motors and generators.

15. SUBJECT TERMS
algorithm, microgrid, power generation, power protection, power quality

16. SECURITY CLASSIFICATION OF:			17. LIMITATION OF ABSTRACT:	18. NUMBER OF PAGES	19a. NAME OF RESPONSIBLE PERSON (Monitor)
a. REPORT	b. ABSTRACT	c. THIS PAGE			Chad N. Miller
Unclassified	Unclassified	Unclassified	SAR	29	19b. TELEPHONE NUMBER (Include Area Code) N/A

TABLE OF CONTENTS

LIST OF FIGURES

LIST OF TABLES

1 EXECUTIVE SUMMARY

3D printing and additive manufacturing (AM) are rapidly growing technical areas. More affordable options and capability advancements increase the attraction for exploring innovative methods. The potential performance and cost saving benefits indicate AM is a prospective disruptive technology over traditional manufacturing methods. However, there are significant challenges that exist within the breadth of methods and material options. Simple, low cost, and quick projects, i.e. a technical sprint, develop relevant experience prior to investing into higher cost and vital projects. This report covers results and lessons learned from an eight week technical sprint effort. The effort explored various technical areas and challenges needed in order to more proficiently explore AM for electric machines such as motors and generators.

2 INTRODUCTION

2.1 Background

3D printing and additive manufacturing (AM) are rapidly growing technical areas. More affordable options and capability advancements increase the attraction for exploring innovative methods. The potential performance and cost saving benefits indicate AM is a prospective disruptive technology over traditional manufacturing methods. However, there are significant challenges that exist within the breadth of methods and material options. Simple, low cost, and quick projects, i.e. a technical sprint, develop relevant experience prior to investing into higher cost and vital projects. This report covers results and lessons learned from an eight week technical sprint effort. The effort explored various technical areas and challenges needed in order to more proficiently explore AM for electric machines such as motors and generators.

2.2 Scope, Team, Resources, and Acknowledgements

This report covers a collaborative eight week experiential project on 3D printing, assembly, experimentation, and hardware testing of a Halbach array permanent magnet motor. The main performers of the project team consisted of high performing undergraduate students majoring in science and engineering (S&E) at about their first year of their studies. The students were mentored by about six full-time S&E's with various technical specialties. All participants worked part-time on the project. The project seed funds consisted of $5,000 for materials and supplies; all labor, overhead, and most equipment was covered through other means. Wright Brothers Institute (WBI) under an AFRL partnership intermediary agreement (PIA) heavily supported the project. All efforts and this reporting is commensurate with experience and resources available. Student and full-time S&E contributors to the effort with gratitude go to Joseph Althaus, Tommy Baudendistel, Ellisen Blair, Cole Breeding, Bobby Buschur, Thomas Chaney, Justin Delmar, Komi Detti, James DiPaolo, Timothy Haugan, Chad Miller, Tom Mitchell, Nathaniel Peck, Logan Rowland, Mary Ann Sebastian, Alex Sheets, Max Stelmack, Bang Hung Tsao, Zafer Turgut, and Kevin Yost. The contributing team would also like to thank MakeSea.com for use of their 3D printed motor files.

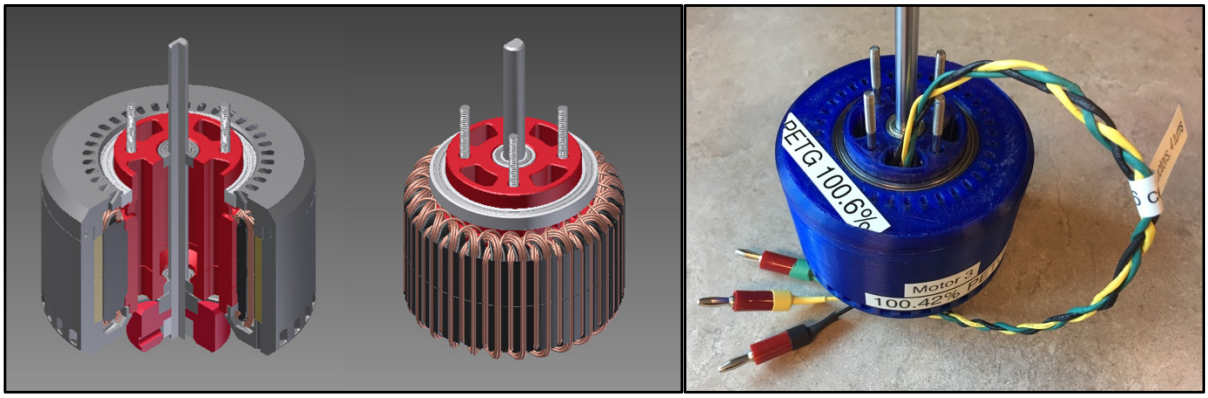

Figure 1 CAD File and Photo of 3D-Printed Permanent Magnet Motor

2.3 Goals and Objectives

Prior to the project, the team challenged ourselves to explore various areas over the eight weeks. Since the design and methods were provided by Makesea.com, we assumed we could accomplish a lot even though we were all working part time. The brainstormed areas included 3D printing the motor parts; machine assembly, magnetic characterization of iron (Fe) filled prints, and design of experiment (DoE) testing of various configurations and design attributes. Significant lessons were learned to prepare for future efforts and covered in the results section of the report. Most areas were completed with appropriate lessons gained, however closing the loop on many of the areas would require additional effort.

Other goals and objectives of the project included (1) experiential training, (2) pioneering a new area at AFRL through a funded seed project, and (3) developing a test-bed for evaluating new materials or designs for electric machines. Designing and fabricating electric machines utilizing traditional electric machine methods is not simple. This is especially true when there is not a current role in AFRL to be a component supplier nor a specific project need which AFRL fills. 3D printing enables a quick and low cost tool for AFRL to affordably build and assemble a motor. The project pioneers a new area for AFRL, not because AFRL will build the machines, but more to create technical acumen and readiness for evaluating and influencing external partners and their concepts.

Moreover, Dr. Randall "Ty" Pollak presented this approach nicely at the 2018 TETS symposium in his talk titled "Metals Additive Manufacturing: Challenges and Opportunities." Dr. Pollak's talk provided reasoning and a plan for "getting-in-the-game:"

- can't be left behind; get in early
- get some additive manufacturing experience before big commitments
- understand your value proposition and hidden costs [1].

This effort and follow-on efforts is a stepping stone for building up a capability in which Dr. Pollak provided a sound blueprint.

3 METHODS, ASSUMPTIONS, AND PROCEDURES

The team purchased the non-commercial use computer aided design (CAD) motor design files from Makesea.com. Creator and designer Christoph Laimer has extensive videos of his motor design and testing methods at his Youtube channel (https://www.youtube.com/user/TheTrueGoofy) [2]. The in-going assumption to the project was that this design has been vetted and would be quick to design and assemble. However, we faced challenges printing some of the intricate designs and the Fe infused plastics. The challenges were overcome after several trials and tribulations and slight design changes. These challenges resulted in delays to the project which affected some of the project overall goals and objectives. Another assumption was that the CAD file could be imported to our FEA software for easy analysis. Likewise, this was only partially true; more analysis with closing the loop for the FEA and hardware testing results is necessary.

The rest of this section will consist of the methods, assumptions, and procedures for various tasks of the project. Areas include printing of various components, magnetic material characterization of the Fe infused printed material, FEA, and hardware testing.

3.1 Methodology

3.1.1 Printed Rotor

Figure 2 The Out-Runner Rotor: The Main Rotor Body with a Permanent Magnet Halbach Array and a Printed Screw-On Cap for Securing the Permanent Magnets

3.1.1.1 Permanent Magnets

There are two magnet sizes to complete the Halbach array – both are Nd52 (NdFeB, Neodymium magnet with magnetic strength figure of merit grade of 52). The large PM is the primary flux contributor which make up the motor magnetic pole. The small magnets allow for relatively efficient flux path connection between the larger pole magnets and also allow for more sinusoidal waveforms. Determining the distribution of magnet weight/mass and magnet field strength was important for physically and magnetically balancing the rotor. The large magnets were measured and then separated into low (<0.70 T), middle (>0.70 T and <0.80 T), and high (>0.80 T) grades based on relative magnetic field strengths, as measured by a Hall effect sensor. The magnetic strengths of the small magnets were measured; we learned there was not a

significant variance in the lot of magnets. We used engineering judgement to determine the small magnets would not be as much of a factor on performance compared to the larger magnets so they were not binned.

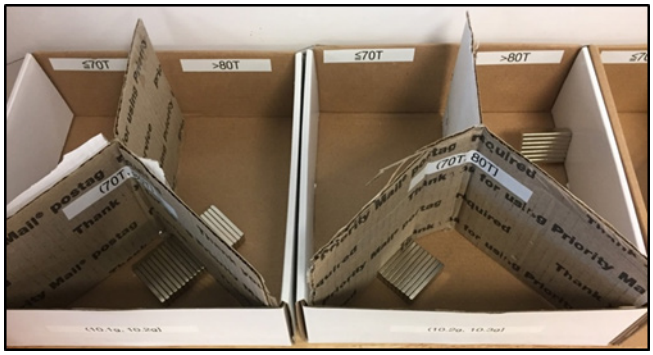

Figure 3 Binning System for Separating the Permanent Magnet by Weight and Magnetic Grade

For measuring the weight and mass of the permanent magnets, careful attention is needed to ensure the magnetic field does not interfere with the measurement system and that the magnet is in the same position for each measurement. Figure 4 shows a photo of a 3D printed jig method used to produce standardized and uniform measurements.

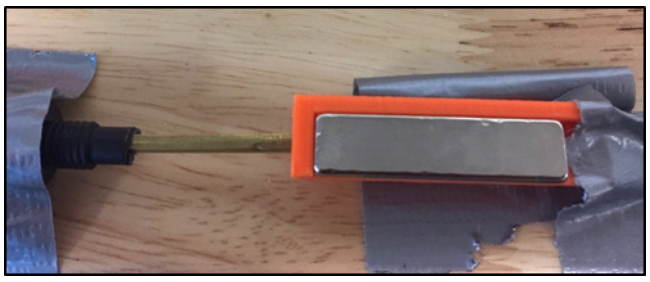

Figure 4 3D-Printed Jig Around the Hall Effect Sensor for Standardizing Magnet Position

3.1.1.2 Permanent Magnet Containment

For our prints, the original design for holding in the magnets was not substantial enough to prevent the magnets from twisting out of the slots during operation. This frequently occurred when the forces generated by interactions of the permanent magnetics and the stator's electromagnet during operation.

An attempted solution was a printed 0.1mm layer cover that was epoxied just inside the open side of the magnet slot. While the magnets were secure, these covers tended to bow out and rub against the stator. Slimming the width and sanding the exterior face were necessary post-processes.

Another solution was to adjust the CAD file of Rotor A to extend the tabs towards each other. This resulted in a lower quality print, with extra material frequently extruded into the magnet slots. If not removed, this material prevented the smaller magnets from seating correctly, which could result in them rubbing against the stator. We did not investigate this further to determine root cause.

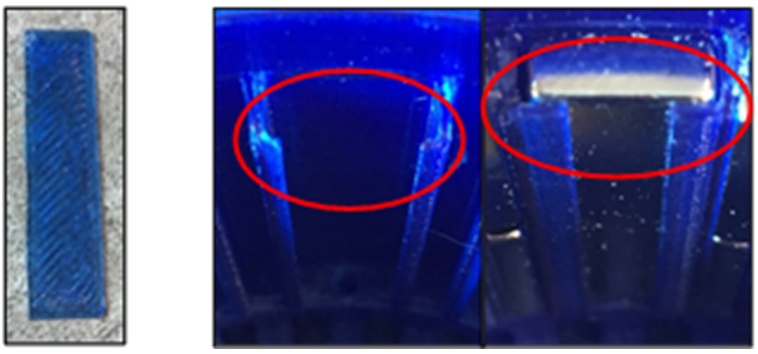

Figure 5 Left is a Magnet Cover, Right is the Original Versus Extended Tabs

3.1.1.3 Dimensioning and Fit

Printed dimensions do not always transfer perfectly from CAD to print. This is primarily due to the real width of plastic filament and shrinkage of the part during cooling. Our primary approach to correcting these dimensions was scaling the part in the slicer. For example, the first rotor print was printed at 100% scale, the inner diameter was measured, and it's percent error from the expected value in the CAD file as adjusted to the scale for the next print (0.42% in the Figure 6 example). This method did not perfectly adjust the dimension to the expected result, but it sufficiently accounted for tolerances. Some features, such as the grooves on the stator mount and any diameter supporting a bearing, needed material removed in CAD.

The most difficult part of tuning the tolerances of the printed parts was maintaining a precise fit between the threads of both rotor halves. The fit can differ between materials. Carbon Fiber Filament (CFF) was the most consistent, being the only material where the main rotor and its cap would screw together with the same scale. Both CPE (Chlorinated Polyethylene) and PETG (Polyethylene Terephthalate) required separate scales for these parts.

Figure 6 Every print labeled with its scaled print value

3.1.2 Stator

For the out-runner motor, the stator is where the armature conductor winding is located. The stator is the inner component where the rotor is on the outer periphery. The armature is the windings in which the electricity is input for a motor or in which electricity is generated into for a generator.

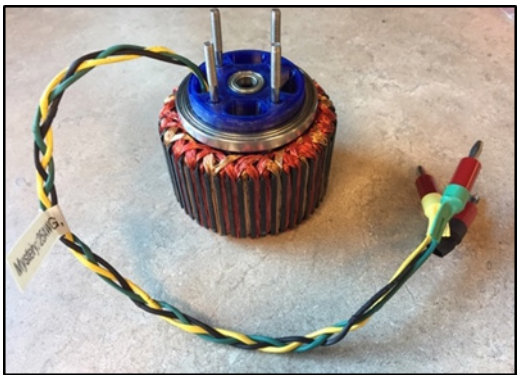

Figure 7 Complete Stator Assembly

3.1.2.1 Wire Armature Conductor and Configuration

The standard motor is wired with 5-meter cables that consists of six 25 AWG enameled copper wires, with 4 turns per pole. Cable was manufactured by twisting together individually cut conductors. To cut the conductors, two posts were secured 5 meters apart. The wire was looped around three times to make a total of six parallel conductor paths traveling from post to post. The ends of the loops were cut, with one secured in a vice and the other twisted 30 times with a drill. The enamel was stripped off the ends of each conductor individually (to ensure complete removal) with sandpaper.

3.1.2.2 Stator Winding

For Wye-configuration, the motor designer recommended soldering one set of ends of each cable together prior to winding. This allows the first phase to anchor the other parts as each is wound. The primary concern with wiring is ensuring the wire will not short to the rotor walls or adjacent windings during operation. Containing wires in the “straightaway” section of the stator simply requires the wire pusher to be slid back and forth in a smooth motion straightening-out the cable after every pass. It is ideal to lay the cable perfectly flat and smooth, with no kinks that take up extra space, to ensure good packing factor and windings that do not protrude into the air gap. When guiding the wire around the stator teeth, ensure the first pass is seated as far as possible into the trench at the base of the tooth (it is fairly easy to lay the cable only partially into the trench). Maintaining a fair amount of constant tension during winding helps fit the cable into the slot. A thin layer of epoxy was applied around the outer circumference to secure the windings from coming loose (ensure it is not corrosive to copper). The leads are fed through three holes in the stator mount underneath the bearing as the stator core slides onto it. Heat shrink was applied around the leads coming from the stator mount, and banana plugs were soldered as connectors.

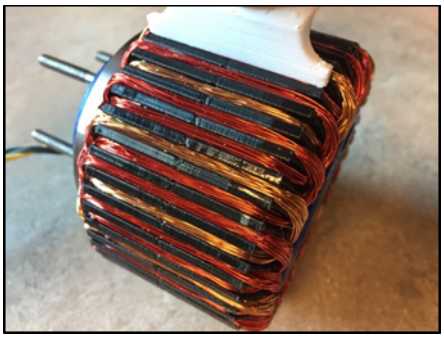

Figure 8 Windings Being Secured with Wire Pusher

3.1.2.3 Wire Configurations

In addition to the standard configuration of the stator windings, several other configurations were assembled and explored:

a) One stator featured cables with half the conductor parallel paths (3 instead of 6 parallel paths) but twice the turns per pole as an attempt to increase voltage and decrease current with respect to each speed.
b) Another winding configuration featured aluminum conductors instead of copper as a material comparison. Aluminum is known to be less conductive (~60%) but less weight than copper (~30%).
c) A third used 22 AWG instead of 25 AWG, with only three conductors per cable (but the same number of turns per pole). This reduced the total area of copper in each slot from 33.93 mm2 to 24.13 mm2, so it is not a great winding configuration for this slot design.

Results of the configurations are covered in the results section.

3.1.2.4 Iron Infused Filament Prints

The stator is designed for “ironfill” PLA (Polylactic Acid) with embedded iron particles for enhanced magnetic conductance. However, the iron particles make the filament brittle and generally difficult to print. A common problem is the extruder gear stripping out a notch in the filament, resulting in the filament getting stuck during the print. Repeated retraction moves the gear back and forth over a small section of filament frequently leads to this failure mode. Lowering the retraction speed and increasing the retraction length reduced this effect, but it only delayed the failure rather than prevent it. Since the stator is a solid print, the best way to reduce retractions is to print with as many shell layers as possible and reduce the area (but not density) of infill, since continuous walls do not require retractions.

After facing the challenges described above, purchasing a new steel nozzle hardware allowed for successful printing of the hard metal, iron infused filament. Not only is steel more physically resistant to abrasive filaments such as Ironfill, but seemingly eliminates clogging of the printer. The reduced thermal conductivity did not affect the quality/appearance of the print when compared to successful brass layers. Once implemented, a steel nozzle made printing effectively flawless with no apparent trade-offs other than the higher cost of the nozzle.

3.1.3 Magnetic Characterization of Printed Iron Infused Plastic Filament

In this magnetic characterization test, five printed toroids and a standard test toroid were measured to find the BH Curve of the materials. The toroids consist of an iron core, two 3D printed with 100% fill, one printed with 100% fill and a 1 mm air gap, and one that was made of the print material in a mold.

The standard test toroid is prewired and set in a box labeled with its primary and secondary windings. The others were wound with a Gorman Productor II Winder. All of them use 22 gauge wire.

The wound toroids are tested on the Remagraph after having the resistance of the secondary windings determined by a fluke. The Remagraph sends a direct current through the toroid and creates a BH curve for each sample. The specifications for each toroid are shown in Table 1.

Table 1 Characterized Magnetic Toroid

Toroid	OD	ID	Thickness	Primary Windings Turns	Secondary Windings Turns	Resistance (Ohms)	H (excitation) (Oe)	Max (J/B)
Standard	2.002”	1.669”	0.260”	250	75	0.3	30	10.0
Iron Core	36 mm	23 mm	12 mm	97	60	1.0	30	5.0
3D Fe Print	36 mm	23 mm	12 mm	100	50	0.9	30	0.02
3D FE Print	36 mm	23 mm	12 mm	97	50	1.0	30	0.05
3D Print w/ 1 mm Air Gap	36 mm	23 mm	12 mm	100	50	1.0	30	0.05
3D Print in Mold	36 mm	23 mm	10 mm	100	50	0.8	30	0.05

In order for the test to be performed these specifications must be entered into the Remagraph.

After putting each toroid through texting, the results can be viewed as various BH curves. The BH curve was only clear in the testing of the standard and the iron core. The printed toroids produced curves with lots of variation and no consistency in curve shape.

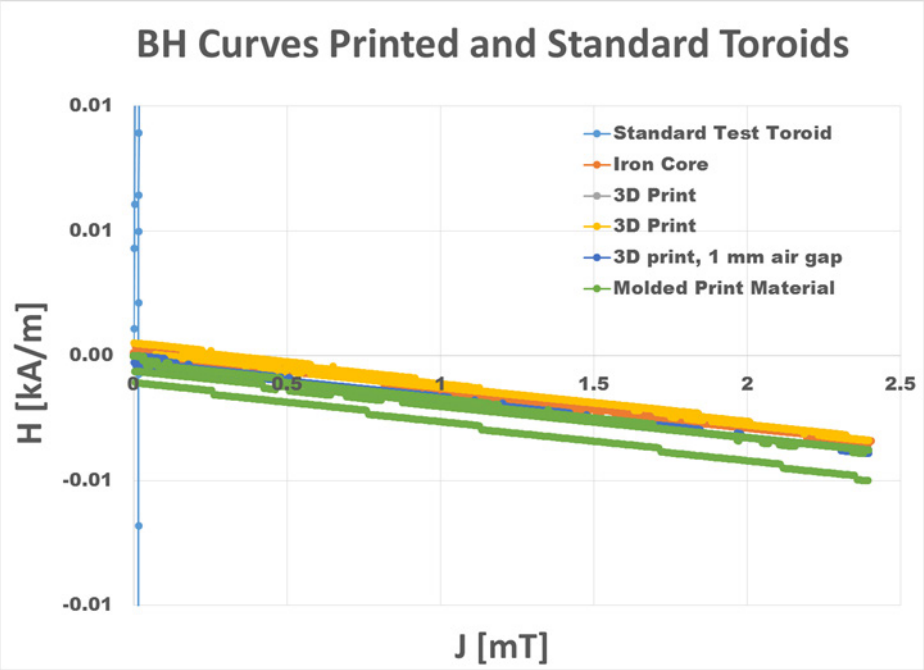

Figure 9 BH Curves for Fe Infused Prints Versus Standard Magnetic Material

The results for the magnetic characterization of the Fe infused filament were not favorable. The ingoing assumption was that it could achieve a relative permeability of 8. A relative permeability of 8 is eight times more magnetically conductive than permeability of free space, though much more loosely. Standard magnetic steels are typically relative permeability of μr = 3000-5000. The steeper the BH curve, the higher the relative permeability. The standard material in Figure 9 shows a zoomed in BH curve for the standard material and it is very steep indicating high relative permeability. While the Fe infused prints was very low and actually negative in relative permeability. The very low permeability could indicate there was not sufficient excitation power of in the characterization equipment necessary to overcome the losses. The negative permeability indicates either the coils were backwards while characterizing, a very low likelihood. More likely for both negative and low permeability is the binding plastic material is exhibiting paramagnetic/diamagnetic traits. The big takeaway is this is not a feasible material and only creates magnetic losses in the component. That said, the absolute value of this BH curve with a μ_r = 1.1 was used for the FEA aspects of the effort.

3.1.4 Finite Element Analysis (FEA)

3.1.4.1 FEA Setup

A two-dimensional model of the generator was created in Infolytica MagNet software. The model contained the following objects with corresponding assigned material properties: rotor and stator (composite Fe-impregnated epoxy, relative permeability of 1), permanent magnets (Nd52 grade), coils (Cu wire). In order to reduce computation resources only a 40° sector was simulated due to periodic symmetry of the system. Electrical circuitry was simulated by connecting each generator coils (phases A, B, C) to individual resistive loads. A transient simulation was performed with different load values, as well as different rotor rotation speeds. Computed

voltage waveforms (measured across the coils) and mechanical torque values were recorded and used to calculate electrical and mechanical power.

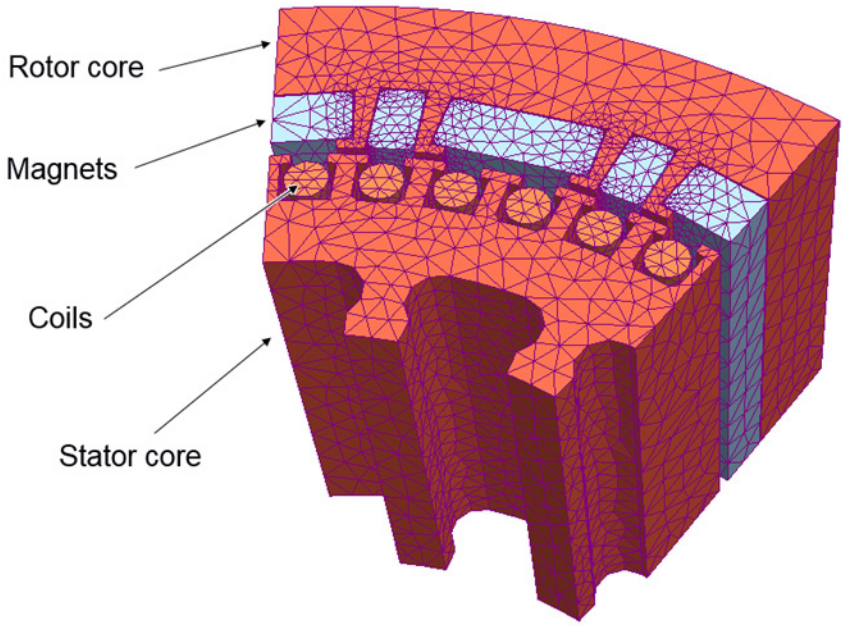

Figure 10 Generator 2D-Model View

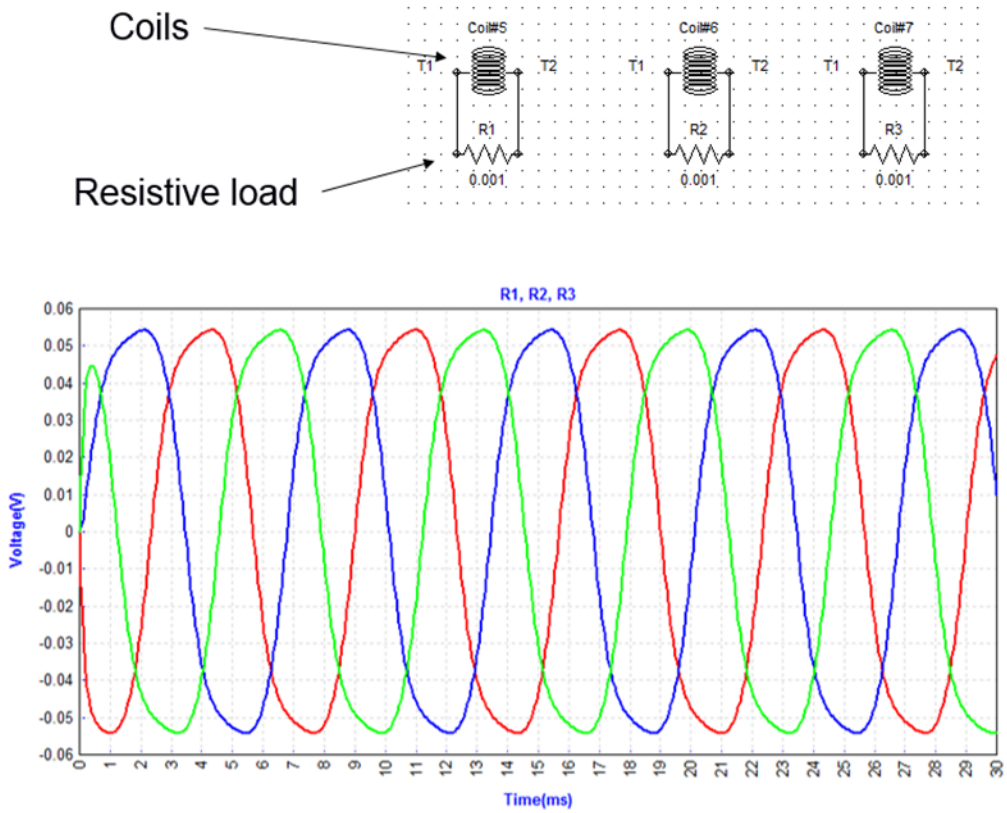

Figure 11 Electric Connection Schematics, and FEA Simulated Voltage Waveforms Across the Generator Coils

3.1.4.2 FEA Simulation Results

The model was simulated at 1000, 3000 and 6000 rpm rotation speed. For each speed setting a variety of resistive loads was used in the range 1 mOhm to 10 Ohm. Calculated voltage peak values and average mechanical torque are shown below (these results are already adjusted for the full circle model since only a 40° sector was simulated), as well as electrical and mechanical power.

Table 2 FEA Results

		Sector model			Full circle adjusted			
Resistance (Ω)	**Speed (rpm)**	**Voltage (V)**	**Torque (Nm)**	**Phase current (A)**	**Voltage (V)**	**Torque (Nm)**	**Pelec (W)**	**Pmech (W)**
10	6000	2.15	0.001	0.215	19.35	0.018	4.2	11.3
10	3000	1.06	0.0003	0.106	9.54	0.0054	1.0	1.7
10	1000	0.355	0.00015	0.0355	3.195	0.0027	0.1	0.3
1	6000	2.12	0.0135	2.12	19.08	0.243	40.4	152.7
1	3000	1.06	0.0065	1.06	9.54	0.117	10.1	36.8
1	1000	0.354	0.002	0.354	3.186	0.036	1.1	3.8
0.1	6000	2.02	0.1325	20.2	18.18	2.385	367.2	1498.5
0.1	3000	1.01	0.066	10.1	9.09	1.188	91.8	373.2
0.1	1000	0.336	0.021	3.36	3.024	0.378	10.2	39.6
0.01	6000	1.365	0.79	136.5	12.285	14.22	1676.9	8934.7
0.01	3000	0.69	0.43	69	6.21	7.74	428.5	2431.6
0.01	1000	0.225	0.146	22.5	2.025	2.628	45.6	275.2
0.001	6000	0.285	1.25	285	2.565	22.5	731.0	14137.2
0.001	3000	0.16	0.89	160	1.44	16.02	230.4	5032.8
0.001	1000	0.054	0.345	54	0.486	6.21	26.2	650.3

3.1.5 Hardware Component Testing

3.1.5.1 Hardware Testing Setup

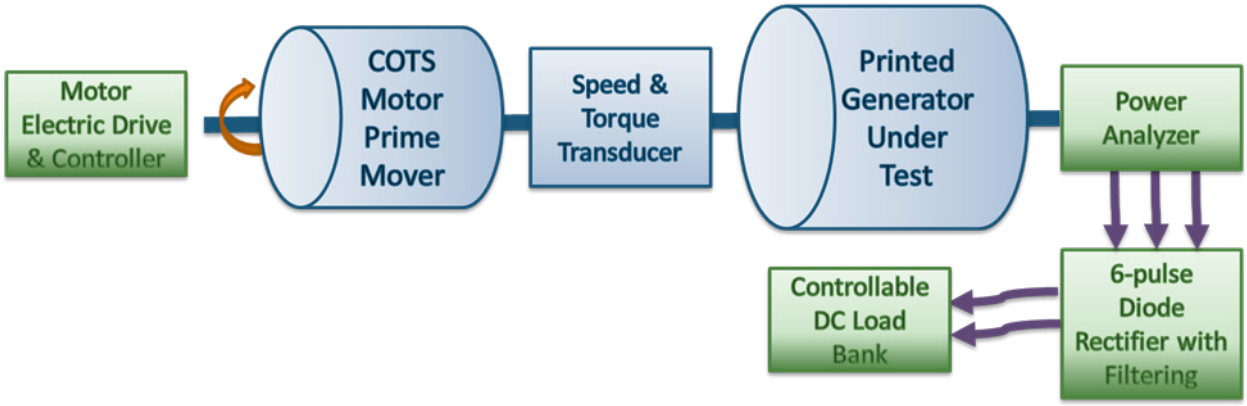

Figure 12 Diagram of Component Hardware Experimental Testing Setup

The experimental hardware testing is important to properly compare various design configuration and material choices. Testing in generator mode without a controller allows for performance characterization of the hardware plant. Testing in motoring mode or generate mode with a controller introduces additional disturbance on the hardware plant which increases variation in results. Therefore, it is recommended to compare these PM machines in open loop generator mode.

This experimental setup included a speed controlled commercial off the shelf (COTS) out runner motor driving the generator, the device under test (DUT). Between the motor and generator is a torque and speed transducer sensor and flexible shaft coupling. The AC power generated was then rectified, filtered, and loaded with a DC resistive load bank. Voltage, current, and phase was measured with an oscilloscope and/or a power analyzer. The qualitative temperature state was also measured with the generator DUT being cooled to nearly the same temperature between each subsequent data point. Finally, care was taken to allow for proper air flow since the machine DUT is fairly enclosed. This air flow must be balanced with proper safety; this setup used a safety shield to isolate the researcher from the custom rotating equipment.

3.1.5.2 Data Acquistion & Performance Calculations

The hardware testing process consisted of measuring mechanicals and electrical performance using a suite of sensing instruments. The oscilloscope, power analyzer, and sensor components are regularly calibrated to their specifications. However, due to the nature of this sprint project and resources, the uncertainty of the data and error was not calculated with any UQ (uncertainty quantification), nor was instrument resolution for the measurements utilized carefully considered. UQ is important in quantifying motor and generator performance since power and efficiency calculations rely on accurate torque, speed, voltage, current, and waveform phase measurements. Poor measurement, utilization of the instrumentation, or poor DAQ setup can result in error propagation and poor quantitative data. Error propagation can easily be seen in the machine efficiency equation since many accurate measurements in the electrical and mechanical domain are needed to achieve an accurate efficiency measurement:

$$Generator\ Efficiency \cong \frac{Voltage * Current * \cos(\varphi)}{Torque * Speed}$$

(Equation 1)

Intuition and judgement can allow us to use the data to compare each DUT to similar experiments since the system and all measurements were taken using the same setup and instrumentation. However, one should be careful since intuition can often be wrong with these types of measurements and calculations. Comparing results at different speeds, current, can result in differing errors for each design point. In conclusion, this report is useful in showing qualitative trends and methods; all quantitative data should be questioned until error is calculated and quantified for each data point.

4 RESULTS AND DISCUSSION

This effort investigated the output performance of various generator design choices through the use of an intuition based DoE (Design of Experiments). The various designs included various grade permanent magnets (PM), conductor type, winding configuration, air gap size, and printed material type.

One qualitative observation was the carbon fiber filament rotor was about 40% less weight than the PETG. The CFF was observed to spin much smoother than the competing heavier plastic. The CFF printed rotor, sample size of 1, was able to achieve 10,000 rpm without noticeable vibrations or concerns whereas there were concerns spinning the plastic printed rotors beyond 5000 rpm.

The CFF also has a larger operating temperature compared to the plastics. The first generator tested used PLA which has a deformation temperature of 40 C It overheated due to insufficient air flow and not monitoring the operating temperature. No failures occurred after increasing air flow and monitoring temperature between tests using a thermocouple.

The first rotor that was tested was Motor 2: CPE rotor, iron fill stator core, default copper winding configuration, mid-grade magnets, and a 0.1mm air gap. It failed when the ironfill stator core began to deform into the air gap and the motor seized at 1000 RPM. However, upon inspection no damage was apparent on the interior of the rotor and the windings were intact. Only the teeth of the stator showed wear. It was later discovered that the deformation temperature of PLA is 40 C, a temperature easily reached during operation. A thermocouple was then installed in every stator to monitor temperature, and a cooling fan was implemented into the testing rig.

Figure 13 Stator Damage Due to Overheating

4.1 Hardware Performance Curves

The data will not be analyzed thoroughly in this report since error and the uncertainty of the data has not been quantified. Further, the ability to make comparisons between configurations is difficult. Figure 14-16 display the open circuit characteristic, the motor torque constant (K_T) curve, and the efficiency curve.

The Back EMF versus speed curve in Figure 14 shows the magnetic circuit characteristic while the generator DUT is driven while driven in no-load open circuit configuration. Since most of the PM machine designs utilize effective air cores, due to little use of soft magnetic steels, the curves are linear with speed. The design with the 8-turn (3-conducutors in a hand) winding configuration clearly shows a different voltage profile than the baseline 4-turn (6 conductors in a hand) designs.

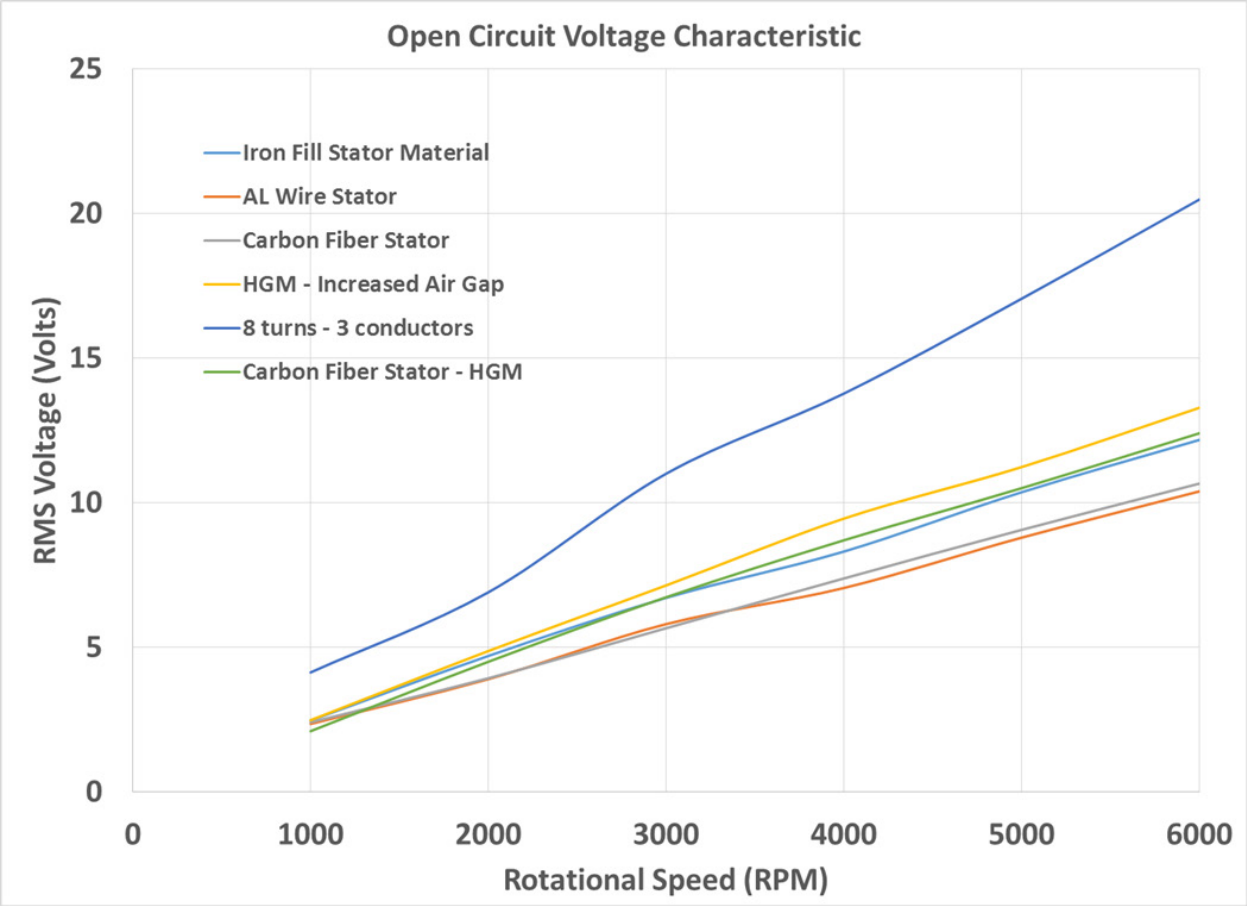

Figure 14 Open Circuit Characteristic Curve

The torque versus current curve in Figure 15 characterizes the electric machine torque constant (K_T). The high turns count armature wound machine again shows a considerably different design. A much smaller current is needed to produce higher torques compared to the other baseline machines. It is assumed the high turn count wound machine would be an interesting configuration if a statistically based DoE was employed.

The aluminum wound machine produced only a slightly lower curve than the copper baseline despite the lower electrical conductivity. It should be noted that aluminum is used for applications in which weight is important but not necessarily volume since Aluminum has ~60% electrical conductivity and 30% the weight of copper. In a design comparing Copper to aluminum, the Al design could increase the volume in the winding of the slot to fit an equal resistance aluminum winding.

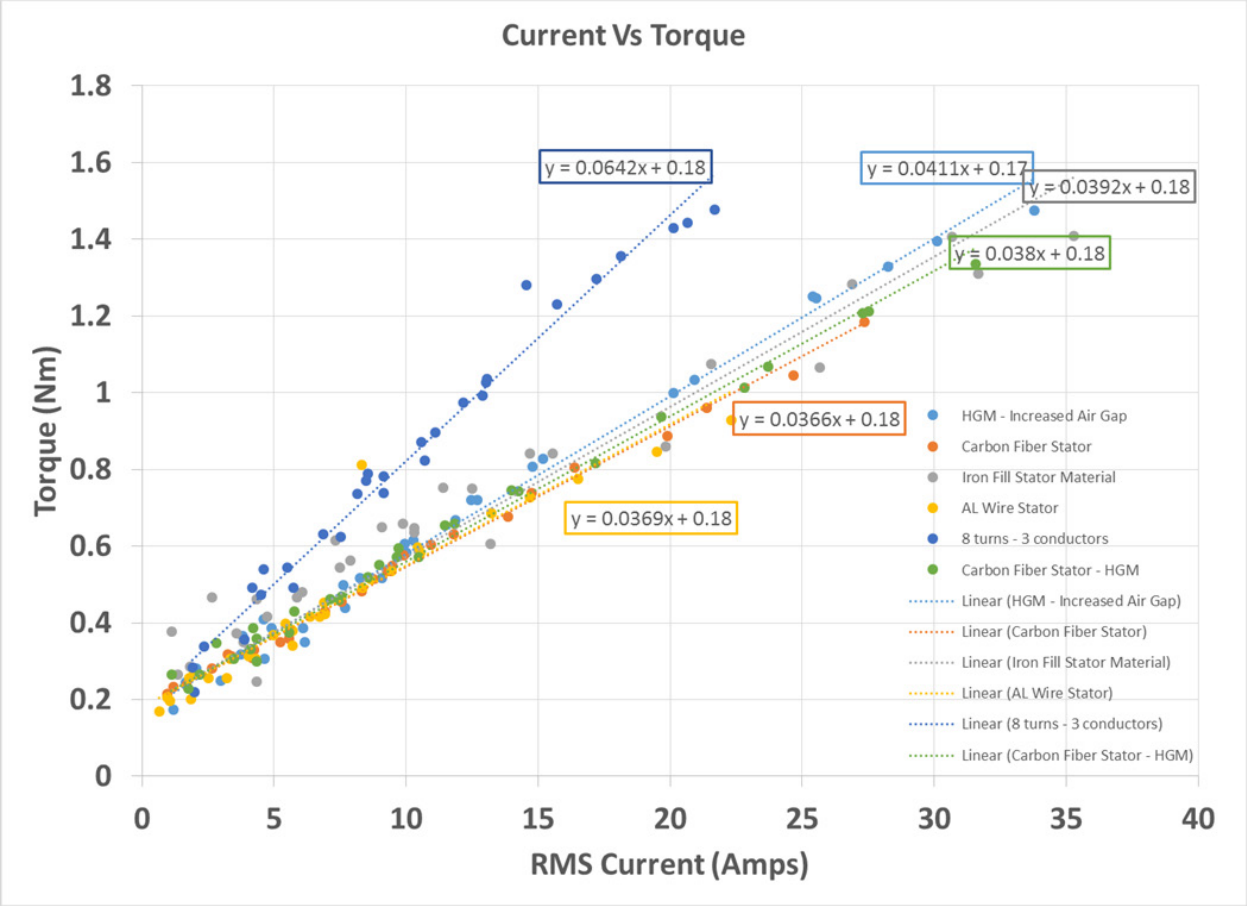

Figure 15 Current Versus Torque

The efficiency of each design is shown in Figure 16. As a reminder, measuring accurate electric machine efficiency is often challenging and caution should be used in measuring various results – see section 3.4.1.2.

There is a notable efficiency hit in the high turn machine compared to the baseline 4-turn generators. The design not intended for the less conductive Aluminum conductors really shows up in the efficiency plot. A new design for Al would be necessary to fairly compare Aluminum with Copper.

The high grade magnet (HGM) with a 50% increased air gap achieved a higher efficiency compared to the baseline machine using medium grade magnets. It is hypothesized that this is due to a more efficient magnetic flux interaction between the rotor and stator. This is one area that could be further studied to understand better.

Finally, the baseline machine of choice utilized carbon fiber filament (CFF) for the stator armature material. As discussed in Section 3.1.3.1, the Iron filled plastic is not a viable design. It is mostly creating core losses in the material without allowing conduction of magnetic flux. Hence, it is mostly only creating losses. The generator DUT where only CFF was utilized, essentially an air-core machine, produced a much higher efficiency machine since there is no

magnetic material to create losses. For this design and current printing constraints, this would be the material of choice.

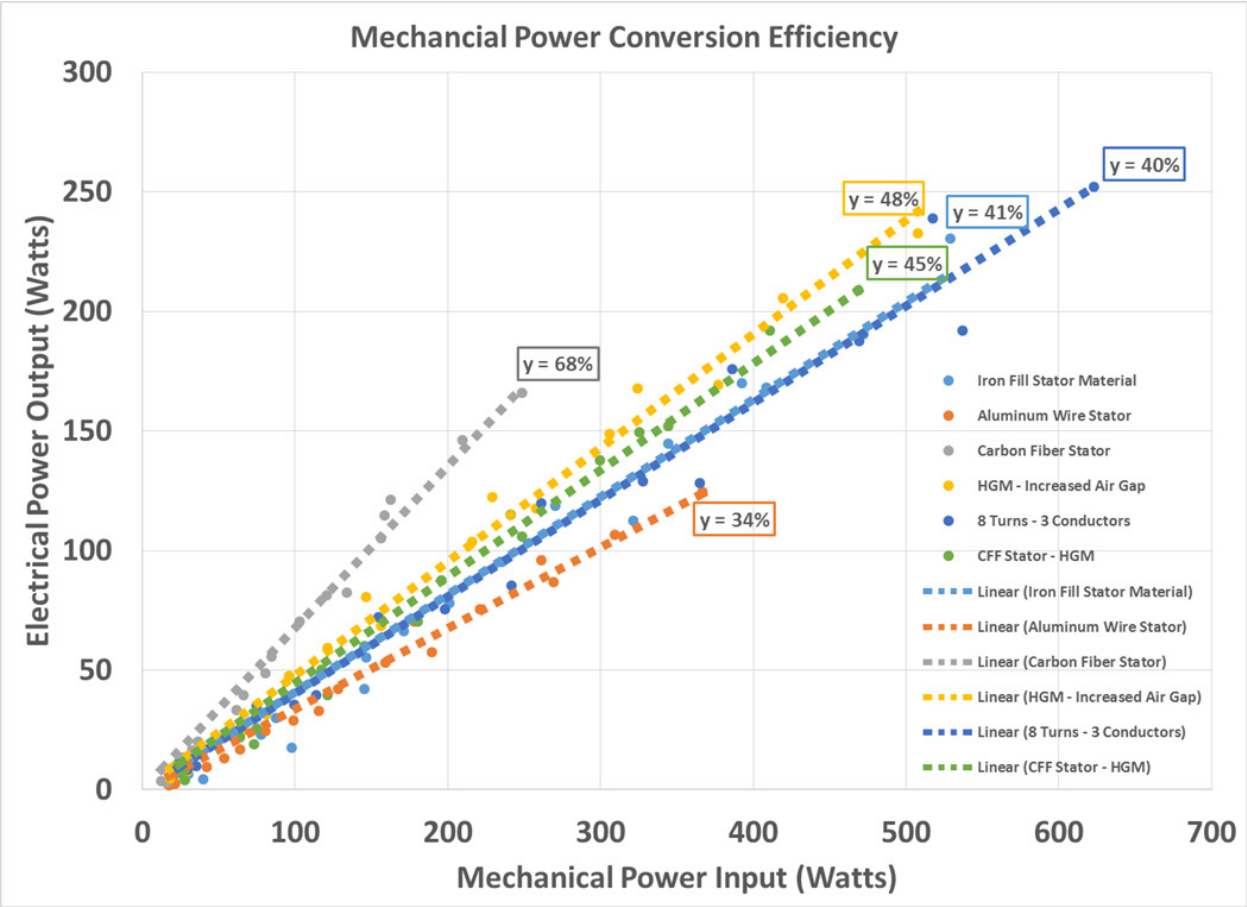

Figure 16 Efficiency for Various Generator Designs

5 REMARKS AND RECOMMENDATIONS

There is significant value proposition for achieving success in additive manufacturing of electric machines. Life cycle cost reduction and increased performance and greatly open up the design envelope not recently achieved in electric machine industry. This project represented a mini seedling effort for "getting in the game" of AM. Many lessons and hidden costs were learned at low cost prior to committing to larger projects. It is recommended to further this effort with a follow on seedling research effort to continue increasing readiness for electric machine innovation. Areas recommended include (1) rapid prototyping, (2) AM of more relevant multifunctional materials employed, and (3) developing a test-bed for advanced materials in electric machines. The follow on effort should be sufficiently resourced to close the loop between design configurations and design of experiments, hardware testing results, and FEA. The below lists a few additional specific takeaways from this 8-week undergraduate student performed effort.

- Carbon Fiber printed rotor spun to 10,000 rpm
- Ironfill print is currently not a viable magnetic flux conductor; relative permeability near that of free space ($\mu_r \cong 1$)
- Printed motor design is a viable test-bed for component analysis; though fair comparisons are difficult (e.g. Al vs Cu conductors)
- Intuition failed on some performance; fair comparisons difficult for single point motor and generator design
- Electromagnetic FEA setup needs more setup than just CAD file and is important for good designs

6 REFERENCES

1. R. D. Pollak, “Metals Additive Manufacturing: Challenges & Opportunities,” Presentation at TETS, 11 September 2018.

2. C. Laimer, Youtube.com channel of various videos for motor design and assembly used in project, https://www.youtube.com/user/TheTrueGoofy.

3. Correspondance from Chris Stavros Makesea.com

LIST OF SYMBOLS, ABBREVIATIONS, AND ACRONYMS

Acronym	Description
3D	Three Dimensional (Printing)
AC	Alternating Current
AFRL	Air Force Research Laboratory
Al	Element symbol for aluminum
AM	Additive Manufacturing
AWG	American Wire Gauge
BH	Magnetic Characterization Curve (B = Magnetic Flux Intensity, H = Magnetizing Force)
CAD	Computer Aided Drawing
CF	Carbon Fiber
CFF	Carbon Fiber Filament
COTS	Commercial off the Shelf
CPE	Chlorinated Polyethylene
Cu	Element symbol for copper
DAQ	Data Acquisition
DC	Direct Current
DoE	Design of Experiments
DUT	Device under Test
EMF	Electromotive Force
Fe	Element symbol for iron
FEA	Finite Element Analysis
HGM	High Grade Magnets
PETG	Polyethylene Terephthalate
PIA	Partnership Intermediary Agreement
PLA	Polylactic Acid
PM	Permanent Magnet
RPM	Revolutions per Minute
S&E	Scientist & Engineer
UQ	Uncertainty Quantification
K_T	Motor Torque Constant
μ_r	Magnetic Relative Permeability